Rev. Roum. Sci. Techn.– Électrotechn. et Énerg.
Vol. **70**, *4*, pp. 477–482, Bucarest, 2025

EFFECT OF DEFECT GEOMETRY IN A COMPOSITE ON RELIABILITY

ZEHOR[1] MOHELLEBI, NOUREDDINE OUDNI[2], OURIDA MEZINE[3]

Keywords: Random geometry and property; Composite; Non-destructive testing; Stochastic finite elements; Reliability analysis.

This work focuses on the study of the effect of the physical properties of a random-type composite material and the geometric shape of defects on the reliability analysis of an inspection device using non-destructive testing. Two types of defect geometries are considered: rectangular and triangular. A stochastic finiteelement method (SFEM) was used to solve the 2D electromagneticequation in a cylindrical structure. The differential sensor recovers the impedance change signal in the fault zone. The signal isanalyzed and compared for the two types of geometries. Post-processing is started to assess the reliability of our structure by determining the reliability index and the probability of failure. The results obtained for random rectangular and triangular shapes are presented, along with a comparison between the stochastic finite element methodand the Monte Carlo method. A good agreement is observed. The results show that the proposed SFEM model offers post-processing in addition to analysis, compared to the Monte Carlo method, which requires numerous draws for analysis and relieson the inverse problem to determine the actual values of the physical property considered.

1. INTRODUCTION

The engineering field, constantly evolving and seeking innovation, is increasingly interested in an emerging material that has become, in a few years, a significant class of advanced materials for high-performance applications: composite materials.

These materials are widely used in various industries, including electronics, electrical engineering, construction, aerospace, and the automotive sector. Composites are now considered a viable alternative to traditional materials, including metals, ceramics, and steel. However, these conventional materials are gradually being replaced by composites due to their many advantages, including their lightweight properties, corrosion resistance, design flexibility, high fatigue resistance, and reduced maintenance costs [1].

A composite material comprises two or more distinct components that are bonded together, complementing each other to achieve superior performance. Reinforcements are embedded in a matrix that serves as a binder. The matrix can be polymer, metallic, or ceramic [1,2].

Composites can come in various structural forms, such as single-layer structures, which consist of one or more identical layers assembled without a specific orientation. Sandwich structures comprise two thin, rigid outer layers enclosing a thick, fragile core. Laminates consist of several layers with fibers oriented according to a defined reference frame [3,4].

However, composite materials are likely to present defects throughout their life cycle despite their advantages. Non-destructive testing (NDT) methods are used for inspection and monitoring to ensure the quality and integrity of materials.

These methods detect and characterize flaws in the composite, such as delamination, porosity, and fiber rupture [5,6].

There are numerous non-destructive testing (NDT) methods, such as ultrasonic testing (UT), radiographic testing (RT), and eddy current testing (ECT), which are widely used for inspection to assess material quality without causing any damage [7–9].

The study of practical systems, such as electromagnetic systems, usually requires knowing the data input to obtain the output information. Physical properties such as electrical conductivity, magnetic permeability, and electrical permittivity must be known at the beginning of problem treatment [10–15].

The shapes of the defects are also needed in the inspection process. In this situation, input data are often used with some uncertainty [15].

The stochastic finite element method has several advantages, particularly in the study and analysis of subsystem sensitivity in a single step [13, 16].

The present work focuses on the study of the reliability of non-destructive testing devices when the defect involves uncertainty in electrical conductivity [17–19] and the defect shape (rectangle and triangle), which are considered random variables and expanded in a series of Hermite polynomials [8,13].

The originality of the intrusive SFEM method used in this study, compared with the reference [14], lies in its direct integration of the uncertainties of several random variables by selecting those to be incorporated into the finite element equations. The polynomial chaos is determined for each type of random variable, and its use is an advanced technique for better numerical efficiency. Implementing the model required reformulating the mathematical model to accommodate the number of random variables to be considered.

The novelty of this study lies in its treatment of two random variables of physical and dimensional nature simultaneously. The calculation code is more robust. It addresses the reliability and the probability of failure for the two geometric shapes of the defect, and comparisons are made. The incidence of the defect's shape has been highlighted.

The stochastic finite element code is developed under the MATLAB package, considering the non-destructive testing technique by eddy currents.

2. STOCHASTIC ELECTROMAGNETIC MODE

2.1. HERMITE POLYNOMIALS

If we consider the variable X of random type, having as input parameters the vector ξ of P independent stochastic variables. It can be shown that if X has a finite variance, then

[1]Electrotechnical Department, MER Laboratory UAMB, UMMTO, Tizi-Ouzou, Algeria. E-mail: zehor.oudnimohellebi@ummto.dz
[2]Computer Science Department, UMMTO, Tizi-Ouzou, Algeria. E-mail: Noureddine.oudni@fgei.ummto.dz
[3]Electrotechnical department, UMMTO, Tizi-Ouzou, Algeria. E-mail: ourida.mezine@fgei.ummto.dz

DOI: 10.59277/RRST-EE.2025.70.4.7

X can be written as a linear combination of multivariate polynomials based on the Hermite polynomials [10,13,20,22]

$$X = \sum_{j=1}^{p-1} a_j H_j(\xi_1, \ldots, \xi_n), \quad (1)$$

p represents the degree of polynomial chaos, $\{H_j(X), j = 0\ldots,\infty\}$ are Hermite polynomials, $\{a_j, j = 0\ldots, \infty\}$ are coefficients of Hermite polynomials where ξ is a reduced centred Gaussian random variable (R.C.G.R.V) with the following density of probability [13–15]:

$$\Phi(g) = \frac{1}{\sqrt{2\pi}} e^{\frac{-\sigma_z{}^2}{2}}. \quad (2)$$

In eq. (1), a_i are unknown coefficients to be determined. We notice that all Hermite polynomials are orthogonal with respect to the Gaussian measure according to the orthogonally property [13]

$$\boldsymbol{E}\left[\boldsymbol{H_{nn}}(\boldsymbol{\xi}(\boldsymbol{\theta}))\, H_{\boldsymbol{mm}}\left(\boldsymbol{\xi}(\boldsymbol{\theta})\right)\right] = 0 \quad \text{if } nn \neq \boldsymbol{mm} \quad (3)$$

Here $\boldsymbol{E}$ [.] denotes the mathematical expectation. For the computation of the coefficients of Hermite polynomials, the work develops the method of projection. Thus, the coefficients of Hermite polynomials are given by the following expression [10,5].

$$a_i = \frac{E[gH_i(\xi)]}{i!} \quad (4)$$

The identification of the Hermite polynomial coefficients in the case of isoprobabilistic transformation is performed using the next formula [13]:

$$a_i = \int_g F_g^{-1}\left(\Phi(t)\right) H_i(t)\, \varphi(t) \mathrm{d}t. \quad (5)$$

2.2. RANDOM GEOMETRY DEFINITION

In the case of random geometry, the two random variables g_{height} and g_{width} of chaos polynomial of order 2 is expressed as follows [8,13]:

$$\begin{bmatrix} g_{height} \\ g_{width} \end{bmatrix} = \begin{bmatrix} a_{01} & a_{11} & 0 & a_{12} & 0 & 0 \\ a_{02} & 0 & a_{12} & 0 & 0 & a_{22} \end{bmatrix} \begin{bmatrix} 1 \\ \xi_1 \\ \xi_2 \\ \xi_1^2 \\ \xi_1\xi_2 \\ \xi_2^2 \end{bmatrix} \quad (6)$$

When g follows a Gaussian law of average $\boldsymbol{\mu_{av}}$ and of standard deviation $\boldsymbol{a_{dev}}$, the calculation of the coefficients of the development (6) is as follows:

$$\boldsymbol{a_0 = \mu_{av}} \quad (7)$$

$$\boldsymbol{a_1 = \sigma_{Dev}} \quad (8)$$

$$\boldsymbol{a_j = 0} \quad \textbf{if} \quad \boldsymbol{j \neq 1}. \quad (9)$$

a_{01}, a_{11}, a_{12} and a_{02}, a_{12}, a_{22} coefficients are obtained from (2), (3) and (4) for each random variable g_{height} and g_{widht}. The projection into the basis of the Hermite polynomials of the dimensions of the defects, the height and the width, leads to [13]:

$$g_{height} = \sum_{j=1}^{p-1} h_j\, H_j(\xi_1, \ldots, \xi_n). \quad (10)$$

$$g_{width} = \sum_{j=1}^{p-1} w_j\, H_j(\xi_1, \ldots, \xi_n). \quad (11)$$

h_j and w_j are the random coefficients of defect geometry to be searched [8].

3. STOCHASTIC SYSTEM CONSTRUCTION

3.1. DETERMINISTIC ELECTROMAGNETIC FORMULATION

The electromagnetic formulation for the deterministic problem is given as follows [13,20]:

$$\overrightarrow{\mathrm{rot}} \wedge \left(\nu_s \overrightarrow{\mathrm{rot}} \wedge \overrightarrow{A_z}\right) + \mathrm{j}\sigma_s \omega \overrightarrow{A_z} = \overrightarrow{J_{sz}}. \quad (12)$$

were: $\vec{A}_z$ is magnetic vector potential magnetic along the z direction; $\omega = 2\pi f$; ν_s – absolute magnetic reluctivity $[\mathrm{H/m}]^{-1}$; f – frequency [Hz]; σ_s – electrical conductivity $[\mathrm{S.m}^{-1}]$; $\overrightarrow{J_{sz}}$: source current density next z [A / m^2].

The finite element formulation leads, considering homogeneous Dirichlet boundary conditions, to the matrix system, whose elements are as follows:

$$[M] + j\omega[N])[A_z] = [F] \quad (13)$$

The elements associated with the matrix and vectors of the system of equations are given by:

$$M_{ij} = \iint_\Omega \nu_s \vec{\nabla}\alpha_i \overrightarrow{\nabla\alpha_j}\, \mathrm{d}\,\Omega, \quad (14)$$

$$N_{ij} = \iint_\Omega \sigma_s\, \alpha_i \alpha_j \mathrm{d}\,\Omega, \quad (15)$$

$$F_i = \iint_\Omega \alpha_i J_{sz}\, \mathrm{d}\,\Omega, \quad (16)$$

$$[\mathrm{A_z}] = \left[A_{z1}, A_{z2,} \ldots\ldots A_{\mathrm{zn}}\right]^{\mathrm{T}}. \quad (17)$$

3.2. PROJECTION OF RANDOM VARIABLES

The projection into the basis of Hermite polynomials of random variables with the combination of eqs. (10) and (11) allow the construction of the stochastic linear system. The non-destructive testing problem of interest is elaborated considering that the current density of the source and the electrical conductivity of the medium are given.

The stochastic linear finite element system is constructed after having carried out the projection into the basis of the Hermite polynomials of the random variables considered below.

The vector potential A_z is the unknown, and the electrical conductivity σ_s . The projection in the basis of Hermite polynomials gives the following expressions [13,15]

$$A_z = \sum_{j=0}^{\mathrm{n_A}} \mathrm{A_{zj}}\, \Psi_j(\xi_1, \cdots, \xi_{\mathrm{M}}), \quad (18)$$

$$\sigma_s = \sum_{i=0}^{\mathrm{n_A}} \sigma_{si}\, \Psi_i(\xi_1) \quad (19)$$

$$n_A = p - 1.$$

By exploiting eq. (10), (11), (18), (19), our stochastic system is obtained as follows [13]:

$$([M^{St}] + j\omega[N^{St}])[A_z^s] = [F^{St}], \quad (20)$$

$$F_k^{st} = \sum_{j=0}^{p-1} \left(M_{jk}^{st} + j\omega N_{jk}^{st}\right) A_{zj}, \quad (21)$$

$$M_{jk}^{st} = x_{0jk} M_0, \quad (22)$$

$$N_{jk}^{st} = \sum_{i=0}^{p-1} x_{ijk}\, N_i^{st}. \tag{23}$$

M_{jk}^{st}, N_{jk}^{st} , F_k^{st} are respectively the random linear matrices and the source vector related to the resolution of the problem, with $k = 0, \ldots, p-1$;

$$C_{ijk} = \frac{i!\, j!\, k!}{\left(\frac{i+j-k}{2}\right)!\left(\frac{j+k-i}{2}\right)!\left(\frac{k+i-j}{2}\right)!} \quad \begin{array}{c} if \;\; i+j+k \;\; pair \; and \;\; k \in [|i-j|, i+j] \\ else \quad 0. \end{array} \tag{24}$$

After integrating all the random, geometric and physical variables given above, we obtain the following algebraic system:

$$L_{jk}^{st} = M_{jk}^{st} + j\omega N_{jk}^{st}. \tag{25}$$

And the associated matrix system:

$$\begin{bmatrix} L_{00}^{st} & L_{10}^{st} & L_{20}^{st} \\ L_{01}^{st} & L_{11}^{st} & L_{21}^{st} \\ L_{02}^{st} & L_{12}^{st} & L_{22}^{st} \end{bmatrix} \begin{bmatrix} A_{z0} \\ A_{z1} \\ A_{z2} \end{bmatrix} = \begin{bmatrix} F_0 \\ F_1 \\ F_2 \end{bmatrix} \tag{26}$$

3.3. ELECTRICAL CONDUCTIVITY

The electrical conductivity of a ply according to referential is expressed by [10,18]:

$$\sigma_{spli} = \begin{bmatrix} \sigma_{sL} & 0 & 0 \\ 0 & \sigma_{sT} & 0 \\ 0 & 0 & \sigma_{sZ} \end{bmatrix}. \tag{27}$$

4. STUDY DEVICE

The study device is a system consisting of a single-layer laminated composite plate (CFRP) with a defect in a differential sensor; the parameters associated with the device are listed in Table 1[12]. The data presented in Table 1 are provided by the JSAEM#Problem1 Benchmark, which was used for the validation of the stochastic finite element model for the CFRP composite [12,15].

Table 1

Parameters of the study device.

Parameters	Value
Coil	
Inner diameter	1.2 mm
Outer diameter	3.2 mm
Height	0.8 mm
width	1mm
Number of turns	140
Current and frequency	1/140 A;150 kHz
Plate	
Height	40 mm
Width	40 mm
Thickness	1.25 mm
Electric conductivity	$\{\sigma_{sL}=5\cdot10^4, \sigma_{sT}=100, \sigma_{sz}=50\}$ S/m
Lift-off	0.5 mm
Rectangular Defect	
Length	10 mm
Width	0.2 mm
Depth	0.125 mm
Triangular Defect	
Base	10 mm
Side	5 mm
Depth	0.125 mm

The finite element method is used when the plate to be tested is a tube. The 2D axisymmetric analysis is appropriate for cylindrical geometries such as tubes, because it simplifies the problem by reducing the dimensionality while capturing the essential characteristics of the material behavior and defects. The study was conducted in 2D axisymmetric as shown in Fig. 1 [12,19]. The characterization of the defect is carried out using the non-destructive testing technique of eddy currents (NDT-EC).

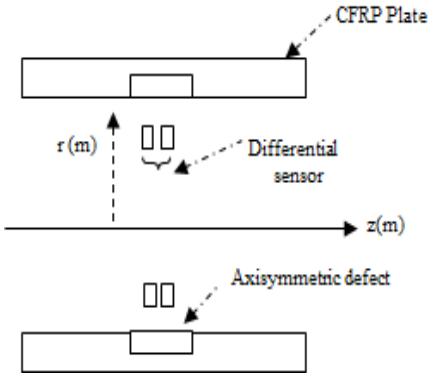

Fig. 1 – 2D axisymmetric NDT-EC device.

After projecting the electrical conductivity σ_{spli} , which is the Gaussian random variable with mean value $\sigma_{splimoy}$ and standard deviation E_{tc}, into the basis of Hermite polynomials, we arrive at the stochastic matrix of electrical conductivity given as follows [14,15]:

$$\sigma_{Spli} = \begin{bmatrix} \sigma_{sL} & \sigma_{sL}\cdot E_c & 0 \\ \sigma_{sL}\cdot E_{tc} & \sigma_{sT} & 2\cdot\sigma_{sL}\cdot E_{tc} \\ 0 & 2\cdot\sigma_{sL} * E_{tc} & 2\cdot\sigma_{sz} \end{bmatrix}, \tag{28}$$

with $\sigma_{sL} = \sigma_{splimoy}$,

The calculation of the impedance is obtained from the electromagnetic energy of the coil,

The number of solutions for *A* and *Z* is equal to p (degree of the polynomial chaos. The formulas for the real and imaginary parts of *Z* are [13–15]:

$$Re(Z) = -\frac{{N_c}^2}{J_{sz}{S_c}^2}\omega \iint_S 2\pi r\, Im(A) dS_c \tag{29}$$

$$Im(Z) = \frac{{N_c}^2}{J_{sz}{S_c}^2}\, \omega \iint_S 2\pi r\;\; Re(A) dS_c \tag{30}$$

The reliability index β is calculated from the limit state function *G*. The latter is obtained from the healthy state of the plate and the solutions obtained in the presence of defects by the stochastic finite element method [8,13,20]

$$\beta = min\sqrt{G}, \tag{31}$$

$$G = Z_0 - \sum_{j=0}^{p-1} Z_j^{i0} \Psi_j(\xi_1, \xi_2)_{max}, \tag{32}$$

where: Z_0 is the impedance of healthy plaque; Z_j^{i0} – impedances with defect from stochastic calculation as a function of the rank of the Hermite polynomial [13–20].

5. RESULTS AND DISCUSSION

This section aims to analyze and evaluate the performance of the system under consideration. By exploiting the

stochastic model constructed with the two random variables, geometry and electrical conductivity, we obtain the following simulation results:

The resolution is done by meshing the domain illustrated in Fig. 2, then the distribution of the magnetic vector potential A for $p = 0$, one of the three stochastic solutions is represented in Fig. 2.

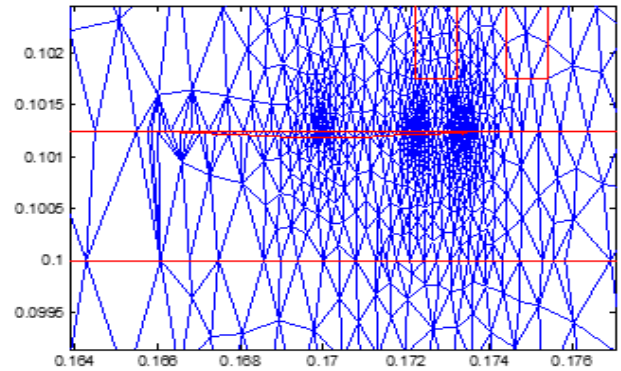

(a)

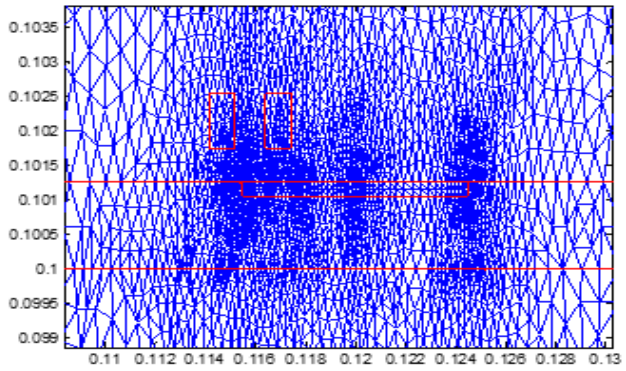

(b)

Fig. 2 – Geometric mesh. (a) triangular, (b) rectangular.

Figure 3 represents the distribution of the magnetic vector potential A, which is the solution of our resolution system. In (a), we observe the behavior of the solution A for a rectangular shape defect, on the other hand in (b), we see the distribution of the vector potential A, for the triangular shape of the defect. The distribution in both cases of geometry is consistent and meets the criteria of the distribution of a magnetic vector potential.

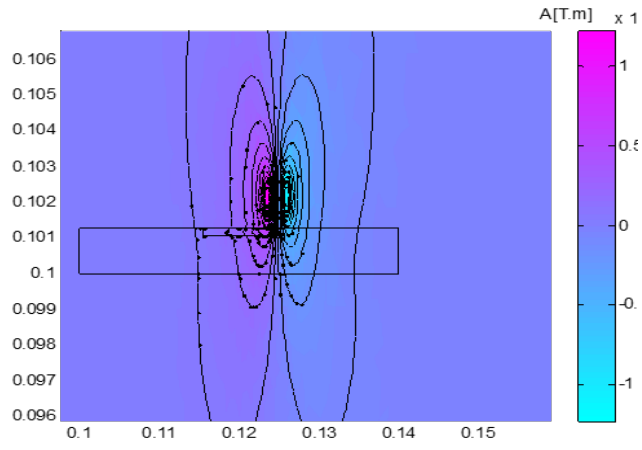

(a)

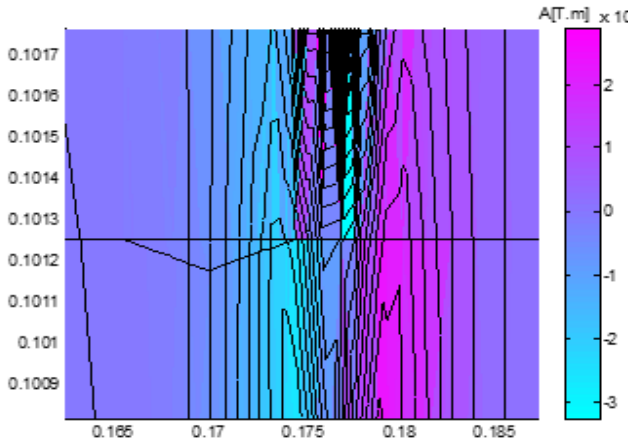

(b)

Fig. 3 – Magnetic vector potential distribution A_0: a) rectangular; b) triangular.

The electrical conductivity is distributed randomly throughout the material for both geometries, with the aim of comparing the influence of the geometric shape of the defect on the variation of the impedance. Figure 4 illustrates this influence. The impedance variation is provided in reduced values between zero and 1 to be able to quantify the difference between the two geometric shapes of the defect. For the triangular shape of the defect, the impedance variation is lower than for the rectangular shape.

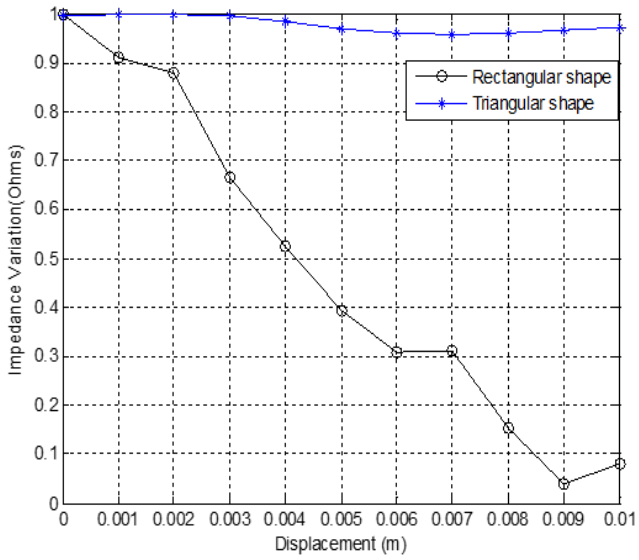

Fig. 4 – Impedance variation for two types of faults.

Figure 5 illustrates the evolution of the reliability index when the sensor moves along the crack. It is noted that the reliability index value is greater than 3 for the triangular geometry. The recommended reliability index value in the absence of defects should be greater than 4 [23,24].

According to Fig. 5, it is noted that the reliability index for the rectangular shape of the defect is less than 3 in most of the defect area, except for the 3 mm and 5 mm distances, which results in a higher probability of the presence of the defect.

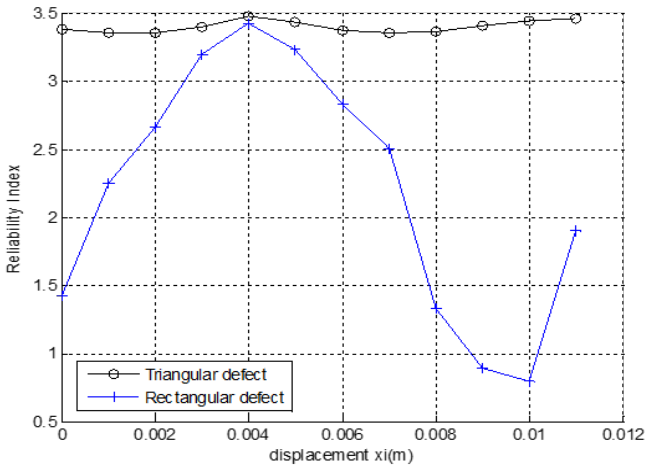

Fig. 5 – Reliability index β for triangle and rectangle defect shape.

Figure 6 compares the evolution of the probability of failure in the zone of the defect for the two types of geometries studied.

The reliability index results obtained for a triangular defect are between 3.35 and 3.50, indicating a very small probability of failure. But when the defect is rectangular, the reliability index is essential and yields a critical value of the likelihood of failure.

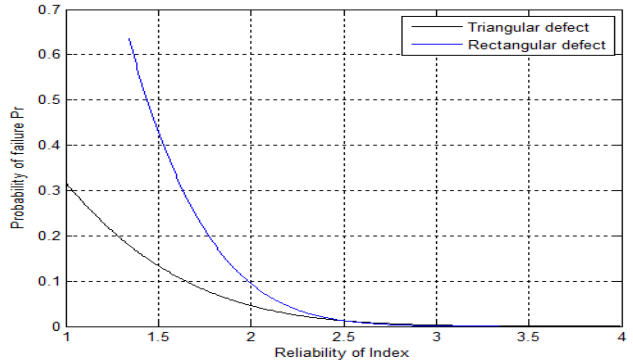

Fig. 6 – Probability of failure for both types of geometries.

6. CONCLUSION

Given the current inspection and characterization of composite materials, the relevance of proposing a defect detection approach led us to develop a stochastic finite element calculation code in a MATLAB environment.

This stochastic approach enables the distribution of electrical conductivity in the suspected area to be represented as a tensor, which is essentially a stochastic matrix. The latter is composed of coefficients calculated from stochastic polynomial chaos. The calculation code enables you to obtain three solutions for a rank of two.

The results obtained for two types of defect geometries enable us to conclude that when the standard deviation is large, the electrical conductivity decreases, as evidenced by a substantial variation in impedance, which characterizes the presence of a defect due to a material deficiency compared to a healthy sample.

The developed stochastic finite element model considers the dimensions of the defect randomly, and simultaneously, the physical parameter, electrical conductivity, is also randomly distributed.

The computation times are extremely short compared to other stochastic methods, such as the Monte Carlo method.

The comparison in terms of computation has been carried out in previously published works whose references are [14,15].

For a single sensor position, the stochastic finite element code simulation consumes 38.21 s of time for 5 810 nodes and 10 955 elements with a PC **Intel Core i5-7500** (3.4 GHz) and 8 GB of RAM. On the other hand, for the same operation with the Monte Carlo simulation, the time is approximately five times longer. Added is the need to go to the inverse problem to recover the input data.

Our stochastic finite element model treats the sensitivity and the probability of failure in a single step.

CREDIT AUTHORSHIP CONTRIBUTION

Author 1 – study design and implementation, development of the computational code, software, and data collection, analysis and interpretation of results, manuscript writing, and supervision.

Author 2 – study design and implementation, development of the computational code, software, and data collection, and manuscript writing.

Author 3 – study design and implementation, analysis and interpretation of results, and manuscript writing.

Received on 4 February 2025

REFERENCES

1. D. Kumar, R. Durgesh, C. Pruncu, *Recent progress of reinforcement materials: a comprehensive overview of composite materials*, J. Mater. Res. Technol., **8**, *6*, pp. 6354–6374 (2019).
2. D. Kumar, S.D. Abdul Kalam, *Design, analysis, and comparison between the conventional materials with composite material of the leaf, springs*, Fluid Mech. Open Access, **3**, pp. 127 (2016).
3. J. Wen, Y. Zeng, C. Wu, J. Guan, H. Guo, *Silk lattice structures from unidirectional silk fiber–reinforced composites for breaking energy absorption*, Adv. Eng. Mater, **22**, pp. 190092 (2020).
4. D. Ragul, V. Thiyagrajan, *A novel fault-tolerant asymmetrical 21-level inverter topology with reduced components*, Rev. Roum. Sci. Techn. – Électrotechn. et Énerg., **68**, *2,* pp. 200–205 (2023).
5. H.K. Bui, G. Wasselynck, D. Trichet, G. Berthiau, *Application of degenerated hexahedral Whitney elements in the modeling of NDT induction thermography of laminated CFRP composite*, IEEE Trans. Magn., **52**, *3* (2016).
6. M. Bowkett, K. Thanapalan, *Comparative analysis of failure detection methods of composite materials, systems*, Syst. Sci. Control Eng., **5**, pp. 168–177 (2017).
7. K. Guerraiche, A.B. Abbou, L. Dekhici, *Intelligent fault detection and location in electrical high-voltage transmission lines*, Rev. Roum. Sci. Techn. –Électrotechn. et Énerg., **69**, *3*, pp. 269–276 (2024).
8. Z. Oudni, A. Berkache, H. Mehaddene, H. Mohellebi, J. Lee, *Comparative study to assess reliability in the presence of two geometric defect shapes for non-destructive testing*, Przegląd Elektrotechniczny, **95**, *12,* pp. 48–52 (2019).
9. J. García-Martín, J. Gómez-Gil, E. Vázquez-Sánchez, *Non-destructive techniques based on eddy current testing*, Sensors, **11**, pp. 2525–2565 (2011).
10. G. Wasselynck, D. Trichet, J. Fouladgar, *Determination of the electrical conductivity tensor of a CFRP composite using a 3-D percolation model*, IEEE Trans. Magn., **49**, *5* (2013).
11. D. Hachi, N. Benhadda, B. Helifa, I.K. Lefkaier, B. Abdelhadi, *Composite material characterization using eddy current by 3D FEM associated with iterative technique*, Adv. Electromagn., **8**, *1* (2019).
12. T. Takagi, M. Hashimoto, H. Fukutomi, K. Miya, H. Tsuboi, M. Tanaka, J. Tani, T. Serizawa, Y. Harada, E. Okano, R. Murakami, *Benchmark models of eddy current testing for steam generator tube: experiment and numerical analysis*, Int. J. Appl. Electromagn. Mater., **5**, pp. 149–162 (1994).

13. Z. Oudni, M. Féliachi, H. Mohellebi, *Assessment of the probability of failure for EC nondestructive testing based on intrusive spectral stochastic finite element method*, Eur. Phys. J. Appl. Phys., **66***, 3,* pp. 30904 (2014).
14. Z. Oudni, T. Mahmoudi, *Exploitation of the spectral stochastic finite element model for the evaluation of surface defects of the CFRP composite*, Prog. Electromagn. Res. M., **127**, pp. 75–83 (2024).
15. T. Mahmoudi, Z. Oudni, A. Berkache, J. Lee, *Characterization of defects in composite materials by the intrusive stochastic method using the Gaussian type random variable*, Przegląd Elektrotechniczny, **99**, *3*, pp. 246 (2023).
16. S. Makkapati, S. Ramalingam, *Lifetime prediction of single-stage LED driver circuit using Bayesian belief network*, Rev. Roum. Sci. Techn. – Électrotechn. et Énerg., **68***, 4*, pp. 351–356 (2023).
17. B. Ponnuswamy, C. Columbus, S.R. Lakshmi, J. Chithambaram, *Wind turbine fault modeling and classification using cuckoo-optimized modular neural networks*, Rev. Roum. Sci. Techn. – Électrotechn. et Énerg., **68**, *4*, pp. 369–374 (2023).
18. M. Khebbab, M. Feliachi, E.H. Latreche, *Application of finite elements heterogeneous multi-scale method to eddy currents non-destructive testing of carbon composites material*, Eur. Phys. J. Appl. Phys., **80**, pp. 10401 (2018).
19. Y. Mizutani, A. Todoroki, Y. Suzuki, K. Mizukami, *Detection of in-plane and out-of-plane fiber waviness in unidirectional carbon fiber reinforced composites using eddy current testing*, Composites Part B, **86**, pp. 84–94 (2016).
20. M. Berveiller, B. Sudret, M. Lemaire, *Stochastic finite element: a non-intrusive approach by regression*, Eur. J. Comput. Mech., **15**, *1-2-3*, pp. 81–92 (2006).
21. A. Efremov, O. Karpenko, L. Udpa, *Generalized multifrequency fusion algorithm for defect detection in eddy current inspection data*, NDT & E Int., **129**, *3,* pp. 102654 (2022).
22. S. Pranesh, D. Ghosh*, A FETI-DP based parallel hybrid stochastic finite element method for large stochastic systems*, Comput. Struct., **195** (2018).
23. M. Loeve, *Probability theory I,* Springer-Verlag Inc. (1977).
24. C.R.A. Da Silva Jr., A.T. Beck, E. Da Rosa, S*olution of the stochastic beam bending problem by Galerkin method and the Askey-Wiener scheme*, Latin Am. J. Solids Struct., **6**, pp. 51–72 (2009).